Journal of Electromyography and Kinesiology 49 (2019) 102364

Contents lists available at ScienceDirect

Journal of Electromyography and Kinesiology

journal homepage: www.elsevier.com/locate/jelekin

EMG map image processing for recognition of fingers movement

Ivan Topalović[a,*], Stevica Graovac[b], Dejan B. Popović[c,d]

[a] Institute of Technical Sciences of SASA, Knez Mihailova 35/IV, Belgrade, Serbia
[b] Faculty of Electrical Engineering, University of Belgrade, Bulevar kralja Aleksandra 73, Belgrade, Serbia
[c] Serbian Academy of Sciences and Arts (SASA), Knez Mihailova 35, Belgrade, Serbia
[d] Aalborg University, Fredrik Bajers Vej 7, Aalborg, Denmark

ARTICLE INFO

Keywords:
Finger Movements Recognition
Array Electrodes
Image processing
EMG maps
Spatial and temporal model
Delicate movements

ABSTRACT

Electromyography (EMG) is the conventional noninvasive method for the estimation of muscle activities. We developed a new image processing method for the recognition of individual finger movements based on EMG maps. The maps were formed from the EMG recordings via an array electrode with 24 contacts connected to a multichannel wireless miniature digital amplifier. The task was to detect and quantify the high activity regions in the EMG maps in persons with no known motor impairment. The results show the temporal and spatial patterns within the images during well-defined finger movements. The average accuracy of the automatic recognition compared with the recognition by an expert clinician in persons involved in the tests was 97.87 ± 0.92%. The application of the technique is foreseen for control for an assistive system (hand prosthesis and exoskeleton) since the interface is wearable and the processing can be implemented on a microcomputer.

1. Introduction

Movements in a healthy human are the consequence of muscle activities that follow a series of neural events in the central and peripheral nervous system. Electromyography (EMG) is a conventional method for assessing the level of muscle contractions. The EMG signals are strongly correlated with the contractile activity generated by the muscle analyzed (Bigland-Ritchie, 1981). The EMG signals are an accessible interface for controlling artificial extremities because they directly reflect the intention of the user at the subconscious level to perform a motor function. (e.g., hand prosthesis (Cipriani et al., 2008; Castellini and van der Smagt, 2009)) exoskeletons (Kiguchi et al., 2004; Lenzi et al., 2012), and robotic manipulators (Fukuda et al., 2003). The EMG signal can also be used as the biofeedback for enabling the training of the motor skills (Giggins et al., 2013).

In many cases, the analysis of EMG is based on multichannel recordings of signals with respect a reference electrode, i.e., unipolar EMG (Kleine et al., 2000; Zwarts and Stegeman, 2003). The other technique is a multichannel recording of voltages between two electrodes over a single muscle (bipolar EMG). Configuration and conventions for the bipolar recordings are described in detail in the SENIAM project (Stegeman and Hermens, 2007). Various signal processing techniques of the conventional EMG were presented in the literature, and some of those have been translated with relative success for control of artificial upper and lower limb prostheses. The major problems are: low level of reproducibility from day to day, relative shift of the positions of electrodes vs. the sources of the signal, and the temporal changes of the surface EMG signals recorded. Huang and Chen, 1999 showed that the combination of Integrated EMG, Variance, Wilson Amplitude, Bias Zero-Crossing, Waveform Length, and 2nd order Autoregression provides a high hand gesture recognition (identification success 85%). The Short-Time Fourier Transform and Short-Time Autoregression were found not to be appropriate for gesture recognition. Results presented by Boostani and Moradi, 2003 indicates that the energy of wavelet coefficients and cepstrum coefficients give better results compared with other 17 features. Since the EMG is a stochastic signal, the neural networks applied on raw or processed EMG signals received much attention (e.g., Artificial Neural Network (Liu et al., 1999), Multi-Layer Perceptron Neural Network (Soares et al., 2003)). However, none of the presented methods provided the satisfactory universal solution.

A solution suggested for reducing the variability of the output based on EMG are the multichannel recordings via electrode-arrays (Mesin et al., 2009). The signals recorded via multi-contact array electrodes allow the analysis of the temporal and spatial distribution of muscles activities (Farina et al., 2008). Previous studies show the two main directions of multichannel EMG analysis. The decomposition of EMG signals to analyze particular motor unit (MU) activations in muscles

* Corresponding author.
E-mail address: ivan.topalovic@itn.sanu.ac.rs (I. Topalović).

https://doi.org/10.1016/j.jelekin.2019.102364
Received 26 May 2019; Received in revised form 6 October 2019; Accepted 8 October 2019

demonstrated advantages of using array electrodes vs. bipolar measurements (Gazzoni et al., 2004; Merletti et al., 2008; Kleine et al., 2007). The high-density (HD) EMG map and analyzing the spatial distribution of electrical activity (Rojas-Martínez et al., 2012; Fang et al., 2015) was another substantial proof of the advantages of the mapping of EMG based on array-electrode recordings. Rojas-Martínez et al. (2013) presented that features extracted from EMG maps recorded on the surface of the forearm and upper arm are provided recognition of movement with accuracy above 95%. The study of Rojas-Martínez et al. analyzed only the isometric contractions for four different hand imaginary movements (wrist flexion, extension, supination, and pronation).

In a recent study, criteria for the EMG spatial and temporal analysis have been defined in detail (Afsharipour et al., 2018): the inter-pad distance within the electrode array should be less than 10 mm to provide the HD EMG map.

The task of our research was to develop a robust method for analysis of EMG signals recorded with the electrodes that are easy to done and a wearable low-noise signal amplifier with wireless communication. We selected to analyze muscle synergies represented by the EMG envelopes. We showed, in our previous study, that the EMG signals recorded via a 24-pad array electrode with the inter-pad distance of about 15 mm could be transferred into images that are detailed enough for global analysis of muscle synergies (Topalović and Popović, 2016). The applicability of the method was later confirmed for the selection of the points for functional electrical stimulation (FES) leading to functional movement of individual fingers and useful grasp/release functions (Popovic Maneski et al., 2016; Popović Maneski and Topalović, 2018).

We present here a new method for the recognition of individual finger movements based on the image analysis of the map constructed from the recordings via a surface 24-pad array and a wearable digital amplifier. The method is based on the hypothesis that the images of EMG activities are highly correlated to the finger movements.

2. Methods and instrumentation

2.1. Electrodes

The skin was cleaned before the electrode placement. The rectangular custom-designed electrode array (12x6cm, 6x4 = 24 circular conductive pads, a diameter of the pad D = 10 mm, interpad distances: 14 mm longitudinal and 20 mm transversal) produced by Tecnalia Serbia, Belgrade, Serbia was used (Fig. 1b). The electrode array was placed on the volar side of the forearm to cover flexor digitalis profundus (FDP) and superficialis (FDS) with the longer side along the forearm. The distal end of the array was one-third of the distance between the wrist and elbow from the wrist. The central line of the electrode was in the middle between the ulna and radius bones. We applied AG702 conductive gel (Axelgaard, Manufacturing Co., Ltd., Denmark) over the circular conductive pads. We used pre-gelled Ag/AgCl electrodes (GS26, Bio-medical Instruments, MI, USA) for the reference electrode and the pre-gelled Pals oval electrode (Axelgaard, Manufacturing Co., Ltd., Denmark) as the ground electrode. The ground electrode was placed on the bony part of the elbow, and the reference electrode was placed between the array electrode and the wrist, 20 mm along the transversal axis of the electrode array.

2.2. EMG acquisition system

We used the Smarting, small, wearable 24-channel digital amplifier with high impedance differential amplifier at the input (gain A = 24) followed by the 24-bit A/D converter (Fig. 1c). The Smarting sends data to the host computer by a Bluetooth protocol. The proprietary software, available from the manufacturer, was used for visual inspection and storing of the data. The sampling rate was set to 500 samples per second (Hz) because the Bluetooth communication channel does not allow a broader range. We validated that the described EMG system is appropriate for the task of this research by analyzing the correlation between the envelopes and the spectra of signals recorded with the system described and the professional analog EMG amplifier (Biovision, Wehrheim, Germany) and connected to the computer via A/D card with 16 bit resolution and sampled at 2 kHz (Topalović et al., 2015).

2.3. Movement assessment

We recorded kinematics data by a custom-designed data glove (Fig. 1a) with six Flex Sensors 4.5″ (Spectral Symbol, Salt Lake City, UT, USA) connected to the 2nd host computed through a National Instruments NI USB-6009 A/D card (Malešević et al., 2012, Popović Maneski et al., 2013). Four sensors were used to measure the flexions of the thumb, index, middle and ring fingers, and two sensors for measuring the wrist deviations. We omitted to measure the flexions of the pinky finger based on the assumption that they are highly correlated with the flexions of the ring finger.

2.4. Data synchronization

The EMG recordings and kinematics data from two computers were synchronized by the Lab Streaming Layer (LSL) system (https://github.com/sccn/labstreaminglayer).

2.5. Subjects

Six subjects with no known sensory-motor impairment signed the Informed consent approved by the ethics committee of the Medical School of the University of Belgrade (age: 27.5 ± 2.3 years, height: 188 ± 6 cm, weight: 84 ± 7 kg, forearm length 32.5 ± 2.5 cm, forearm circumference 26.5 ± 1 cm) participated in the study. We recorded the EMG from the dominant right forearm in all six subjects. We present data from three subjects: two out of five who were well-coordinated, and one that was somewhat clumsy.

2.6. Procedure

A subject was sitting in front of the table with the forearm and palm resting on the table. The first auditory signal was the command to the subject to raise the hand and forearm, keeping the wrist angle stable and the palm facing the table. The second auditory signal was the request that the subject sequentially flexes, keep it flexed for a short time (≫0.5 s) and extends the finger back to neutral (finger by finger) as shown in Fig. 2. The recording session was repeated ten times, with 5 s rests between the flexions. The maximum EMG that the subject can generate was recorded in a separate session: subjects were asked to flex finger as strong as they could (all four fingers).

2.7. Preprocessing and generation of the EMG maps

The signals were processed offline in Matlab (Mathworks, Natick, MA, USA). We applied 3rd order Butterworth high pass filter at 30 Hz to minimize the shift of the baseline and reduce the impact of motion artifacts. We applied for 5th order Butterworth notch filter to reduce the noise at 50 Hz. We generated EMG envelopes of the absolute values of EMG signals by using 5th order Butterwort low pass filter with cutoff frequency at 2 Hz. All envelopes were normalized relative to 40% of maximal voluntary contraction (MVC). We selected the value 40% after heuristic analysis of recordings, which suggested that the range of EMG is much below the EMG during MVC.

EMG maps were obtained in 5 steps (Fig. 3):

1. On-line generation of the EMG envelopes for all channels (at each point of time 24 values of the EMG envelope);
2. Testing if any of the envelopes crossed the threshold at 0.05 (2% of MVC). If the test was positive, the program moves to the next step,

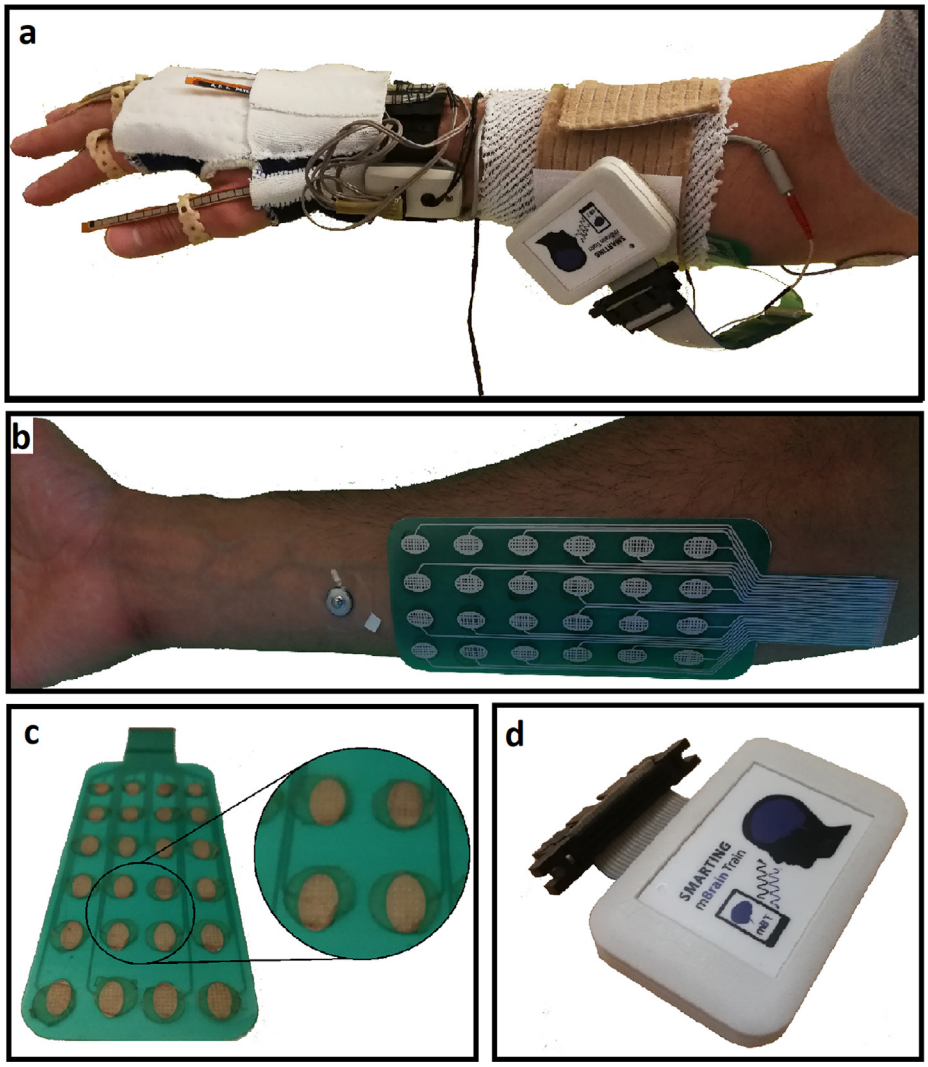

Fig. 1. a) Experimental setup; b) Position of the array electrode; c) 24 pad array electrode (Tecnalia Serbia, Belgrade, Serbia) with AG702 conductive gel (Axelgaard, Manufacturing Co., Ltd., Denmark); d) 24 channel Smarting wireless amplifier (mBrainTrain, Belgrade, Serbia).

and if not, then step 1 is repeated. The low value 2% was selected because of the task to detect the onset of muscle activity as fast as possible and the fact that 2% corresponds to the white noise. The 2% threshold was found to be applicable for all users based on the thorough heuristic analysis of two experts.

3. Forming a 24-point map (nodes in the 6x4 matrix) matching the pattern of the pads on the electrode;
4. Applying the bicubic (spline) resulting with the interpolation (31 points between every two points of the original matrix);

2.8. Extracting the Features

Extracted features are related to the intensity and spatial distribution of electrical activity of muscles. As original EMG maps were obtained of EMG envelopes which had been normalized relative to MVC, values in all EMG maps are represented in the absolute color scale (ASC), common for all EMG maps. Each ACS-EMG map was scaled based on max–min normalization relative to the current maximal and minimal value in the map forming the relative color scale (RCS) (Fig. 4b). We applied 2D H-dome transform to detect the regions of high activities around local maximums in an RCS-EMG map in (Fig. 4c). 2D H-dome transform is based on translating the surface of EMG map, represented in a 3D coordinate system (x and y coordinates represent the position of pixels, and z coordinate represents the intensity), down the z-axis for height "h." We decided to set parameter h to the value 0.1 (10% of the global maximum in each map) after heuristic analysis of the recordings in all subjects. Each local peak of the translated surface represents the level for the unique threshold for each elevation of the surface around the local maximum. The intersection of thresholds and RCS-EMG map forms a binary mask with detected areas of high intensities. We applied morphological opening to a binary mask to clear detected small objects (less than 20 pixels) which are not of interests. We used the binary mask to original EMG mask to extract regions of highest activities and their intensities (Fig. 4d).

For each detected object, we calculated the position of local maximum, and its intensity, calculated as the volume of the object shown in Fig. 4e. To calculate the volume, we used 2D trapezoidal numerical integration. Each object was described with three parameters: x and y coordinates of local maximum expressed in the number of pixels and volume expressed in arbitrary units. For further classification, we calculated volume ratios of the four most significant objects as:

$$R_i = \frac{V_i}{\sum_{j=1}^{4} V_j}$$

where the volume of the i-th object and is the relative contribution of the i-th object.

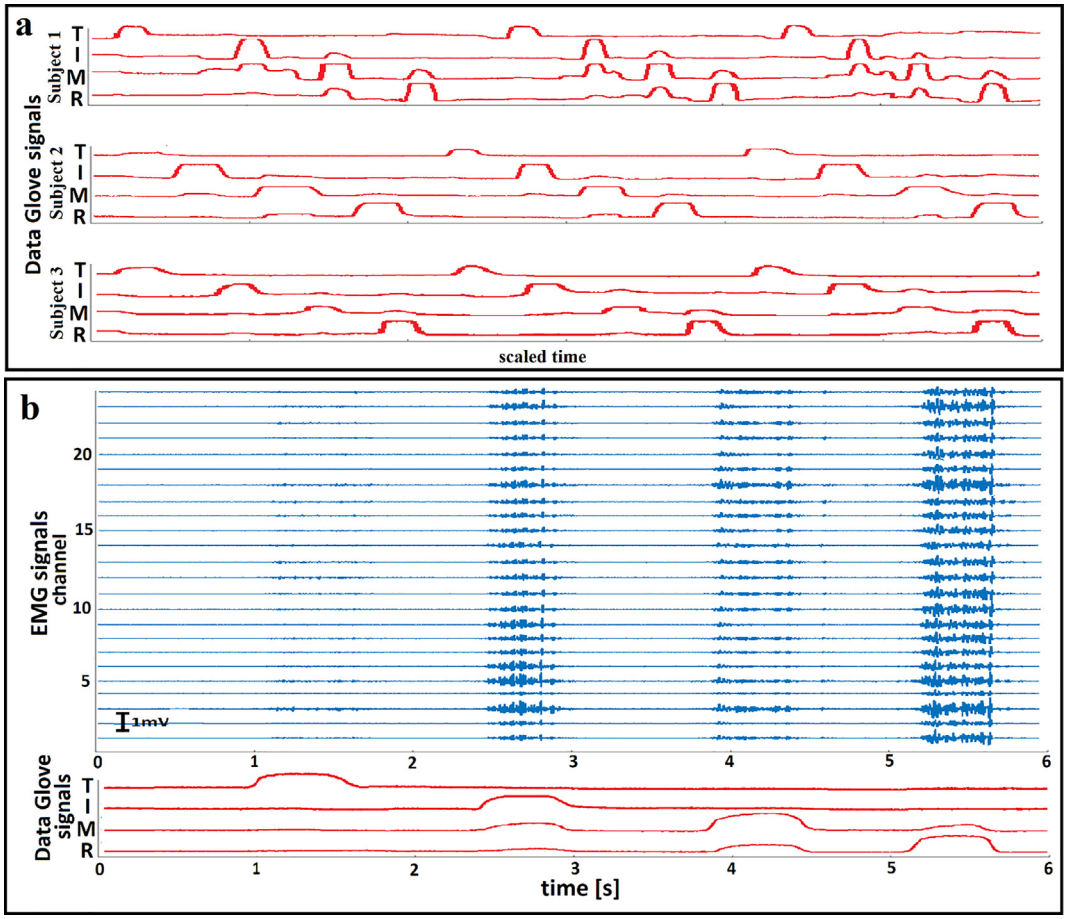

Fig. 2. a) Joint angles recorded by the Data Glove signals for three subjects. Subject 1 was not able to separately flex individual fingers, while the other two representing the other five subjects performed the task efficiently. b) Example of recorded signals (subject 3) during sequential movements with the thumb, index, middle, and ring finger. The top panel presents 24 EMG signals recorded on the volar side of the forearm. The bottom panel shows kinematic signals recorded by Data Glove.

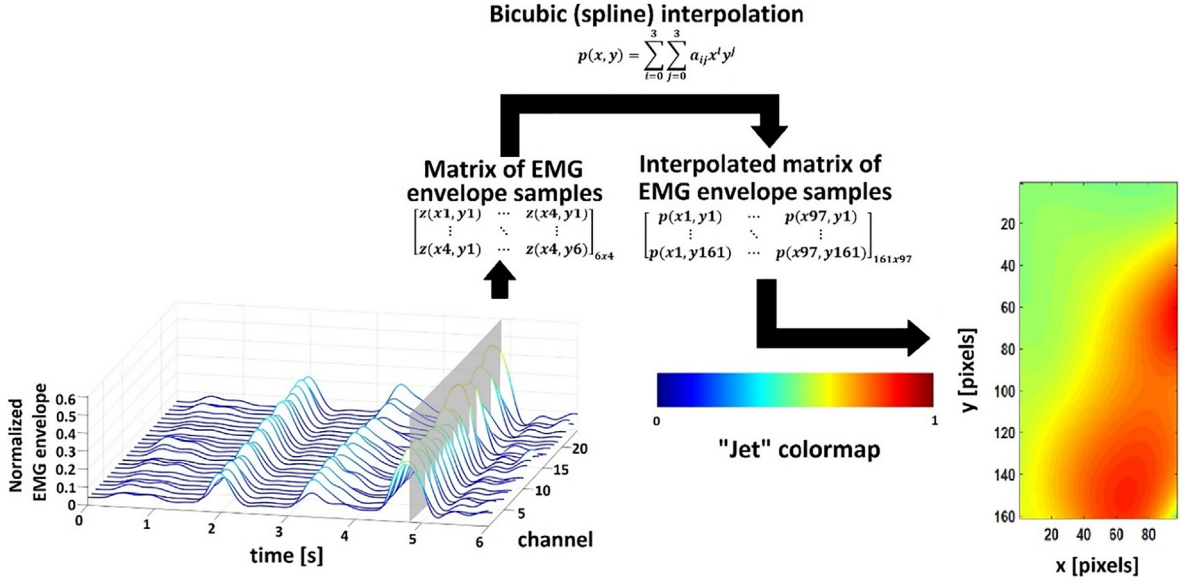

Fig. 3. The five-step procedure of forming the EMG maps: 1) collecting the current values of the EMG envelopes from each channel (24 samples of EMG envelopes; one per channel); 2) checking if any envelope was above the threshold at 0.05 (2% of MVC). If the result was yes, then the program moves to the next step, and if not, then the program returns to step 1 to collect new samples; 3) organizing the collected samples into a 6x4 matrix to match the layout of the recording array electrode; 4) applying bicubic (spline) interpolation by adding 31 points between each two points in the original matrix; 5) assigning the colors (standard "jet" colormap in Matlab) to the appropriate values in the matrix (0 – deep blue, 1- deep red). (For interpretation of the references to color in this figure legend, the reader is referred to the web version of this article.)

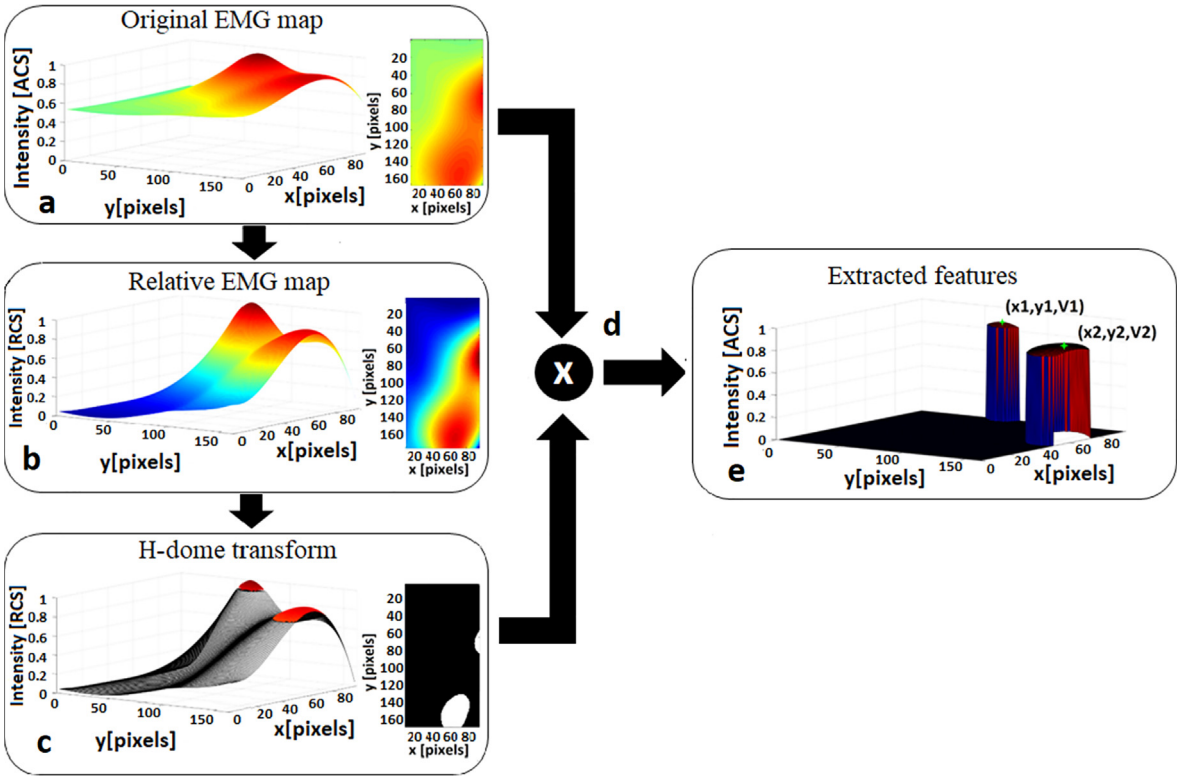

Fig. 4. The procedure of features extraction of the EMG map: a) ACS-EMG map (right) and the same map in the 3D coordinate system (x and y-axis -number of pixels, z-axis – Intensity in ACS); b) scaled original map in RCS (right) and the same map in 3D coordinate system (x and y-axis -number of pixels, z-axis – Intensity in RCS); c) Result of the implementation of H-dome transform on RCS-EMG map and estimation of the high-intensity zones around the local maximums (red areas in left figure) and binary map with marked pixels of the zones (white pixels (logical 1) are representing the detected zones); d) the multiplication of binary map and original ACR-EMG map; e) the extracted features – coordinates of local maximum (x, y) and volume of the object (V). (For interpretation of the references to color in this figure legend, the reader is referred to the web version of this article.)

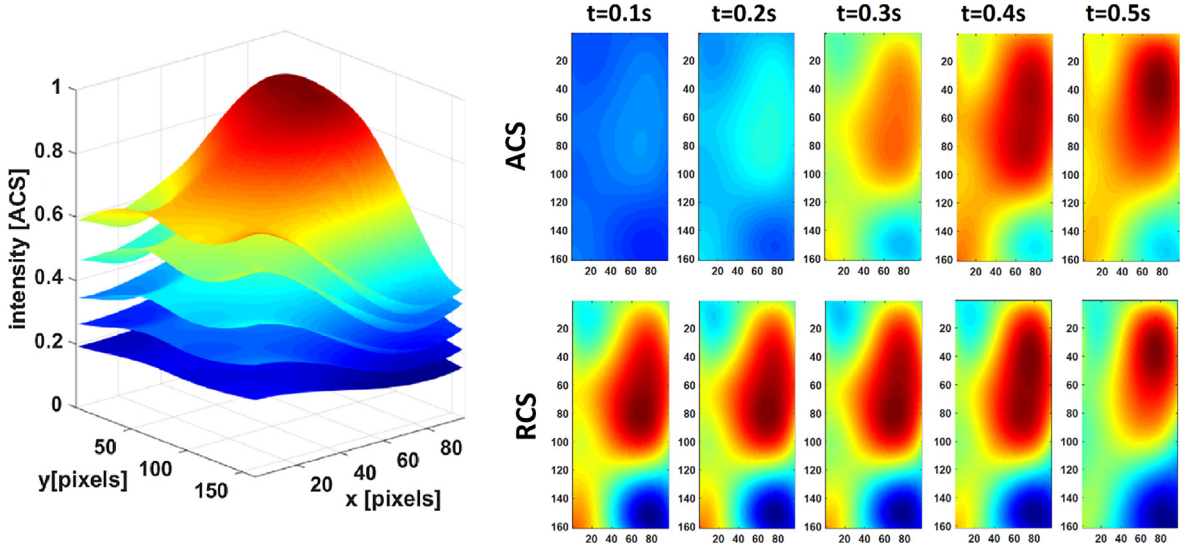

Fig. 5. Comparison of ACS and RCS maps in time in 3D space. RCS-EMG maps (left panels) provide information about the current ratio of high-intensity regions producing the more stable objects compared with ACS - EMG maps (right panel); thus, simplifying the detection process.

2.9. Classification

Each map was described by a set of the parameters of four most significant objects (4 × 3 matrix, each row represents one object, and columns are x coordinate y coordinate and volume). Number four was selected after a detailed analysis for all six-subjects who participated in the study. The visual analysis of the EMG maps during the finger movements clearly indicated four regions with significant activity. This was the reason to decide that four is the number of targets for the classification. If an object was missing, then all the parameters for that object were set to 0. The orders of the objects in the matrix were based on the minimal Euclidean distance between the object and the upper left corner of an EMG map and the minimum Euclidian distance between the object from the new EMG map and mean position of

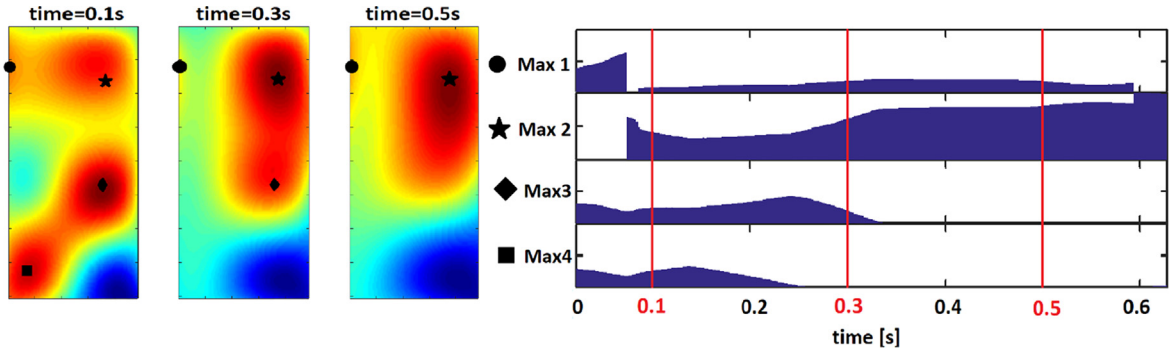

Fig. 6. Four characteristic local maxima detected during a single movement. Three left panels are EMG maps (RCS) at different times. The circle, star, diamond, and square show the mean positions of the local peaks. The intensities of the areas surrounding the local maxima are in right panels/ Red lines indicate the times for the maps presented in the left panel. The explanation of the discontinuities is presented in the text. (For interpretation of the references to color in this figure legend, the reader is referred to the web version of this article.)

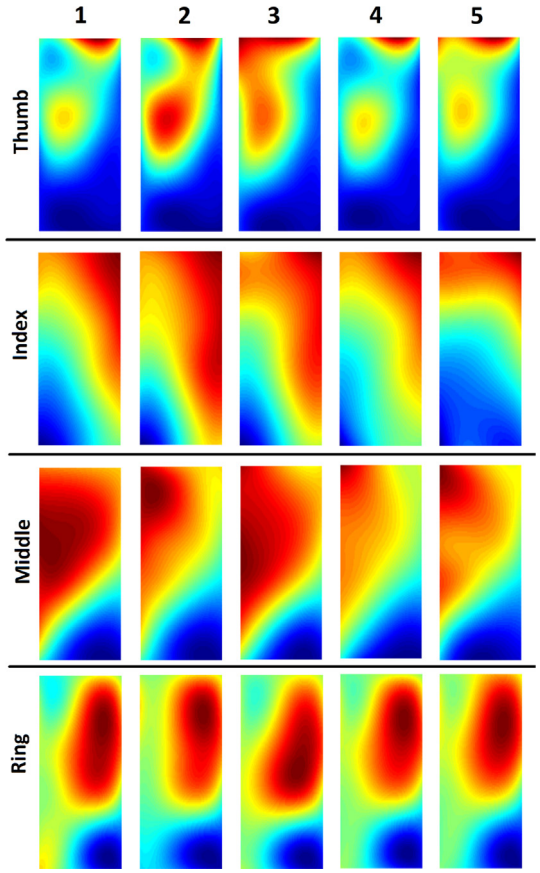

Fig. 7. EMG maps recorded in the same subject (relative color scale - RCS) for the thumb, index, middle, and ring finger (top row) for five repetitions of the same task. The maps are not identical as expected, but the objects remain at the same positions.

previously detected objects. We applied an additional condition that the gap between the new object and the previous object was less than 30 pixels.

We considered the intervals of EMG activity when only one-digit flexion/extension was determined from the data glove signals. These periods include 4000 samples each. For each subject, we formed data set of 4000 samples (12 × 4000 matrix, 1st four for x coordinates of local maximums, 2nd four rows for y coordinates, and 3rd four rows for the volume ratios). We separated the data into 70% for the training and 30% for the testing. We used the cross-validation for the performance evaluation. The second test was to use the sequences of 1500 samples and apply cross-validation for each subject.

We tested different classification methods (K nearest neighbor - KNN, Support Vector Machine - SVM, various types of decision trees - DT). All of the classification methods have high performance. We selected to use the cubic K nearest neighbor (KNN) method because the highest accuracy for the set of data was obtained for the data we recorded in the tests. We used K = 10 tested after trying several values (from 10 to 100), and the overall accuracy changed for only 3%, while the computing time increased much. The use of KNN was effective since our data does not include extreme values, such as movements of two or more fingers. The use of KNN could be a limitation for the cases when two or more fingers are moving since it would be challenging to deal within the area of the feature map. The evaluation of these more complex movements was left for later studies.

3. Results

The top panel (blue) in Fig. 2 shows an example of 24 EMG signals recorded during sequential movements of the thumb, index, middle and ring finger, and the bottom panel (red) shows kinematic signals recorded synchronously.

Fig. 3 shows the process of creating the EMG maps from EMG envelopes recorded from the volar side of a forearm. The matrix formed of 24 envelope samples provides a sharp pixel-type image of electrical activity under the pads. The more detailed matrix (161x97) obtained after applying the bicubic (spline) interpolation offers the more accurate approximation of the electrical activities under the array electrode. The numerical values in the matrix are in the range [0,1] in the ACS scale due to the MVC normalization.

Fig. 4a shows an example of the EMG map, also shown in Fig. 3, represented in a 3D system, where the z-axis represents the intensity of the EMG map, and x and y coordinates show the geometry. Features which adequately describe the regions in the EMG maps are coordinates of local maxima and quantification of the intensities of these areas.

The sizes and intensities of the regions depend on the recruitment levels and the distance between the muscle and electrode (skin). During a functional movement, the level of muscle contraction, its length and shape, and the position relative to the electrode varies; thereby, ultimately, the EMG map changes. The changes in EMG maps complicate even more the classification of movements; yet, the relatively large size of contact pads and the distances between those reduce the variability. Due to small variations in position and length of forearm muscles during a movement compared to dimensions of electrodes, these variations have a profound influence on the regions in the EMG maps. These variations can be metaphorically described as mountain rocks rising from the sea (Fig. 5, left panel). The position and intensity ratio of the regions (rock peaks) are similar during the same movement with some variations due to complex mechanism of MUs activation and

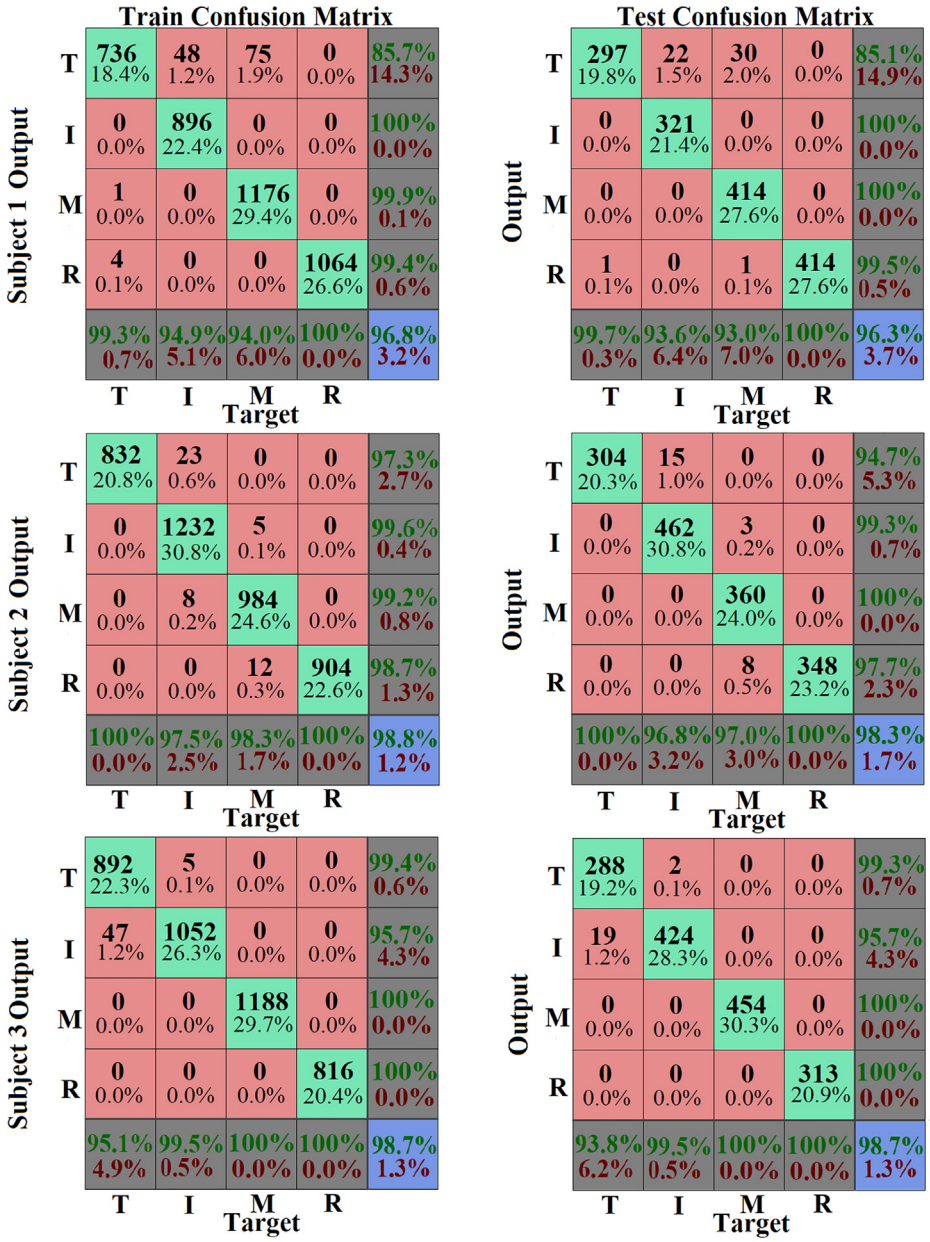

Fig. 8. The confusion matrices for three subjects showing the classification accuracy for each finger individually.

movement of muscles relative to array during a finger flexion. To stabilize the EMG maps for shaping the objects in a digital image, we re-scaled the EMG maps in RCS. Fig. 5 (right panel) shows the result of rescaling. This procedure simplifies the image processing, but the information about the variation of intensity in time is reduced.

Three EMG maps during the same movement at a different time (0.1 s, 0.3 s, and 0.5 s from the beginning of the action) are shown in Fig. 6. Local maxima, characteristic for the movement, are presented with different symbols (circle, star, diamond, and square). Right panels in Fig. 6 show the ratio of object volumes and its change along vs. time. The graphs on the right panel show discontinuities. These discontinuities happen when the centers of activities are relatively close and their intensities are high enough to overlap the areas above certain level that program perceives them as one big area (in the case presented the positions marked with the star and circle at $t \approx 0.07$ and at $t \approx 0.6$ s). More precisely, when the difference between lower local maxima and height of area intersection between two centers is lower than parameter h, h-dome transform can't separate these two areas. This problem can be overcome by using Watershed techniques, but these techniques can lead to over-segmentation (Rojas-Martínez et al., 2012). However, immediately after the intensities get comparable or move apart the algorithm operates correctly. This potential problem was the reason to follow four maxima since the probability that this will be the case in all four areas is very low.

We tested the method in subsequent movements as well as when removing the electrode and repositioning it on a different place. We show the example of EMG maps (relative color scale - RCS) for the thumb, index, middle and ring finger recorded in Subject 3 in Fig. 7. The panels in Fig. 7 show the expected differences in EMG maps from finger to finger and expected variations of EMG maps for different flexions of the same finger, since the flexions are not identical.

Fig. 8 comprises the confusion matrices showing the classification accuracy for each finger individually. One can observe that the recognition of the index finger is the best. One reason is the fact that the distance from the recoding site and the muscle responsible for the flexion is the shortest compared to other distances. The striking result is that the EMG recordings are correlated with the thumb flexion although the electrode was not covering the main thumb flexors. The only

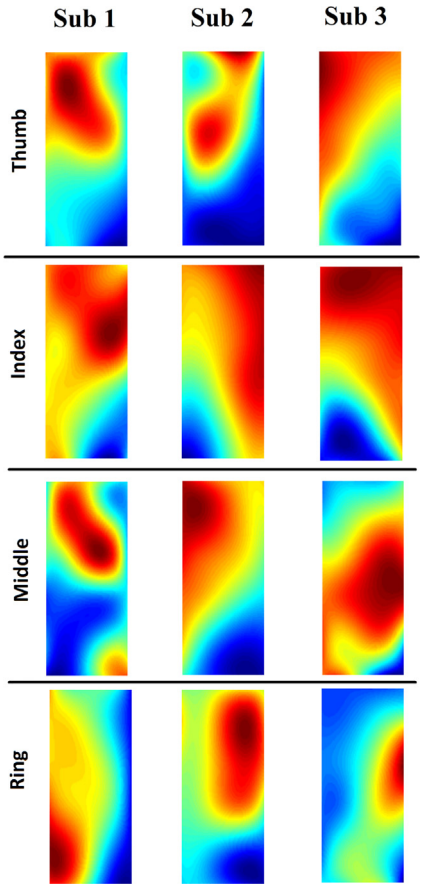

Fig. 9. EMG maps for three subjects described (relative color scale - RCS) for the thumb, index, middle, and ring finger (top row). The differences are expected since the anatomical features, and the movement strategies are different from subject to subject.

explanation we have is that the subjects implemented a motor control strategy where the thumb is a synergist with other finger flexors; hence, the algorithm is classifying the synergy not a simple finger flexion.

We show examples of EMG maps for the same tested task in three subjects (Fig. 9). As expected, the maps are not identical. The differences are due to the anatomical differences and different muscular synergies from person to person. The said finding suggests that the analysis should be performed for each subject if the maps are planned to be used for the control of an assistive system. The mean accuracy for all six subjects was 97.7 ± 1.1% for cross validation (training data) and 97.5 ± 1.3% for the additional validation data.

4. Discussion

We presented data for three subjects from the group of six healthy volunteers. We presented data for two subjects as representatives of the group of five subjects who performed with similar movement dexterity, and data for one subject who was clumsy compared to others during the recording session. We were not able to find the reason why this subject performed with below-average dexterity.

Although the subjects were specifically asked to repeat the finger movements with a similar strength, significant differences in the levels of electrical activities in all channels for different movements were recorded. The differences are the consequence of inherent synergies that subject implement at the subconscious level. Thereby, the EMG recordings differ greatly because of the amount of activation of deep and superficial finger flexors (Fig. 4 and ACS-EMG maps in Fig. 5). When the source of electrical activity (muscle or part of the muscle responsible for the movement) is closer to the surface of the skin, then the intensity of EMG signals would be higher (Roeleveld et al., 1997). These variations in EMG signals measured at the skin make the classification of the muscle activities pattern very difficult, especially when the conventional two-electrode configuration is used. The same is even more expressed if one is to analyze movements involving several fingers in synchrony.

The presented results follow our hypothesis that the spatial component coming from the use of an array electrode provides necessary information about the muscular synergies in the region covered by the array. The use of the array electrode directly lowers the impact of the non-optimal placement of two electrodes in the conventional EMG acquisition (Farina et al., 2001; Mesin et al., 2009). Fig. 6 shows the differences between the locations of high muscle activities, which would be impossible to show from the bipolar recordings.

An essential feature of the use of the array electrode is that signals recorded provide rich information about the synergistic activities. Namely, although the electrodes are covering the forearm and not the region where primary thumb flexors (flexor pollicis brevis m, flexor pollicis longus m, thenar muscle group) are the thumb activity can be anticipated. The activity recorded during flexion of thumb shown in Figs. 4 and 5 originate from muscles synergists being activated to stabilize the wrist and other fingers. The estimated high percentage of classification accuracy for the thumb flexion indicates that features obtained from recordings on synergists can be used t for indirect movement recognition. As said earlier, motor control strategies, i.e., how the individual activates their synergist muscles depends much on many internal and external factors.

The high percentage of classification accuracy for the thumb flexion indicates that recordings from synergists can be used for indirect movement recognition. This placement flexibility and indirect movement recognition are essential for potential implementation for transradial prostheses and exoskeletons. More precisely, the recordings from the preserved muscles in proximal forearm after the amputation could potentially provide control signals for the thumb.

The high classification performances (accuracy > 95%) for different hand movements (Rojas-Martínez et al., 2013) indicates that multichannel recordings, EMG mapping, and spatial-temporal analysis represent a plausible solution for movement recognition. The analysis of the complete synergy of different muscle groups on the forearm and upper arm, by detecting regions of the highest activities in HD EMG maps obtained by EMG recordings with a large number of channels and HD array electrodes provides rich information about movement and muscle activities. The classification performances shown in the confusion matrices (Fig. 8), and overall accuracy of 97.7 ± 1.1% are significant and comparable with the results in Rojas-Martínez et al. (2013). We could conclude that the presented approach in EMG analysis, even when using one array with a reduced number of pads (24 pads) and a wireless wearable amplifier gives a solid basis for the practical applications. EMG maps obtained by using the 24-pad array electrodes and implementation of the interpolation have a sufficiently high resolution for detecting different regions of high electrical activity and discriminates these regions.

It is impossible to directly compare the performances of some other techniques described in the literature since the setups are different. The starting difference is that the literature describes results based on the data acquisition system with high-density electrodes with many more recording channels. In addition, we studied different motor tasks compared with the motor tasks presented in the literature. The reasons that we selected to study the flexion of the fingers relates directly to the plausible use for the synthesis of maps for the selective electrical stimulation of the paralyzed hand opening and closing (Popović Maneski et al., 2016, 2018).

In this presentation we describe only the use of KNN since we learned from earlier tests in our Lab that it has the highest accuracy when compared with SVM and DT, as already set in the Methods. The application of more complex and sophisticated techniques for

classification would provide more features, but the results that we present will not change, meaning that it is possible to study muscle synergies with a relatively simple wearable system comprising 24-channel amplifier and 24-contact electrode with the spacing in range of cm.

Maps represented in the ACS contain the information about intensity variations in time. That is valuable information for estimation of movement force in potential implementations, but at the same time, makes the movement recognition more difficult by constant destabilization of objects in EMG maps (Fig. 5). RCS-EMG maps provide information about the current ratio of high-intensity regions producing the more stable objects than ACS - EMG maps and simplifying their detection and directly influences the movement recognition accuracy.

In this study, we presented that the classification based on the position of the regions of high activity and their intensity has excellent accuracy for the phases of movements characterized by the constant joint angle (period after finger stopped flexing and before is starts extending). In future research, attention should be paid to transition from one movement to another and from a relaxed state to the first part of the movement. The more complicated issue that needs attention in the future is the case when the movement involves several fingers and wrist in parallel.

References

Afsharipour, B., Soedirdjo, S., Merletti, R., 2018. Eliminating the Bottleneck of sEMG Recordings: array Electrodes. In: International Conference on NeuroRehabilitation, October, pp. 994–998.

Bigland-Ritchie, B., 1981. EMG/force relations and fatigue of human voluntary contractions. Exercise Sport Sci. Rev. 9 (1), 75–118.

Boostani, R., Moradi, M.H., 2003. Evaluation of the forearm EMG signal features for the control of a prosthetic hand. Physiological Measurement 24 (2), 309.

Castellini, C., van der Smagt, P., 2009. Surface EMG in advanced hand prosthetics. Biological Cybernetics 100 (1), 35–47.

Cipriani, C., Zaccone, F., Micera, S., Carrozza, M.C., 2008. On the shared control of an EMG-controlled prosthetic hand: analysis of user–prosthesis interaction. IEEE Trans. Robot. 24 (1), 170–184.

Fang, Y., Liu, H., Li, G., 2015. Zhu X. A multichannel surface EMG system for hand motion recognition. Int. J. Humanoid Robot. 12 (02), 550011.

Farina, D., Leclerc, F., Arendt-Nielsen, L., Buttell, O., Madeleine, P., 2008. The change in spatial distribution of upper trapezius muscle activity is correlated to contraction duration. J. Electromyo. Kinesiol. 18 (1), 16–25.

Farina, D., Merletti, R., Nazzaro, M., Caruso, I., 2001. Effect of joint angle on EMG variables in leg and thigh muscles. IEEE Eng. Med. Biol. Mag. 20 (6), 62–71.

Fukuda, O., Tsuji, T., Kaneko, M., Otsuka, A., 2003. A human-assisting manipulator teleoperated by EMG signals and arm motions. IEEE Trans. Robot. Autom. 19 (2), 210–222.

Gazzoni, M., Farina, D., Merletti, R., 2004. A new method for the extraction and classification of single motor unit action potentials from surface EMG signals. J. Neurosci. Methods 136 (2), 165–177.

Giggins, O.M., Persson, U.M., Caulfield, B., 2013. Biofeedback in rehabilitation. J. Neuroeng. Rehabil. 10 (1), 60.

Huang, H.P., Chen, C.Y. Development of a myoelectric discrimination system for a multi-degree prosthetic hand. in: Proceedings 1999 IEEE International Conference on Robotics and Automation, IEEE; 1999; vol. 99(3). pp. 2392–2397.

Kiguchi, K., Tanaka, T., Fukuda, T., 2004. Neuro-fuzzy control of a robotic exoskeleton with EMG signals. IEEE Trans. Fuzzy Syst. 12 (4), 481–490.

Kleine, B.U., Schumann, N.P., Stegeman, D.F., Scholle, H.C., 2000. Surface EMG mapping of the human trapezius muscle: the topography of monopolar and bipolar surface EMG amplitude and spectrum parameters at varied forces and in fatigue. Clinical Neurophys. 111 (4), 686–693.

Kleine, B.U., van Dijk, J.P., Lapatki, B.G., Zwarts, M.J., Stegeman, D.F., 2007. Using two-dimensional spatial information in decomposition of surface EMG signals. J. Electrom. Kinesiol. 17 (5), 535–548.

Lenzi, T., De Rossi, S.M.M., Vitiello, N., Carrozza, M.C., 2012. Intention-based EMG control for powered exoskeletons. IEEE Trans. Biomed. Eng. 59 (8), 2180–2190.

Liu, M.M., Herzog, W., Savelberg, H.H., 1999. Dynamic muscle force predictions from EMG: an artificial neural network approach. J. Electromyo. Kinesiol. 9 (6), 391–400.

Malešević, N.M., Popović Maneski, L., Ilić, V., Jorgovanović, N., Bijelić, G., Keller, T., Popović, D.B., 2012. A multi-pad electrode based functional electrical stimulation system for restoration of grasp. Journal Neuroeng. Rehabil. 9 (1), 66.

Merletti, R., Holobar, A., Farina, D., 2008. Analysis of motor units with high-density surface electromyography. J. Electromyo. Kinesiol. 18 (6), 879–890.

Mesin, L., Merletti, R., Rainoldi, A., 2009. Surface EMG: the issue of electrode location. J. Electromyo. Kinesiol. 19 (5), 719–726.

Popović Maneski, L., Malešević, N.M., Savić, A., Keller, T., Popović, D.B., 2013. Surface-distributed low-frequency asynchronous stimulation delays fatigue of stimulated muscles. Muscle Nerve 48 (6), 930–937.

Popović Maneski, L., Topalović, I., Jovičić, N., Dedijer, S., Konstantinović, L., Popović, D.B., 2016. Stimulation map for control of functional grasp based on multi-channel EMG recordings. Med. Eng. Phys. 38 (11), 1251–1259.

Popović Maneski, L.P., Topalović, I. EMG Map for Designing the Electrode Shape for Functional Electrical Therapy of Upper Extremities. in: International Conference on NeuroRehabilitation, Springer, Cham. 2018. pp. 1003-1007.

Roeleveld, K., Stegeman, D.F., Falck, B., Stålberg, E.V. Motor unit size estimation: confrontation of surface EMG with macro EMG. Electroencephalography and Clinical Neurophysiology/Electromyography and Motor Control, 1997 vol. 105(3). pp. 181–188.

Rojas-Martínez, M., Mañanas, M.A., Alonso, J.F., Merletti, R., 2013. Identification of isometric contractions based on High Density EMG maps. J. Electromyo. Kinesiol. 23 (1), 33–42.

Rojas-Martínez, M., Mañanas, M.A., Alonso, J.F., 2012. High-density surface EMG maps from upper-arm and forearm muscles. J. Neuroeng. Rehabil. 9 (1), 85.

Soares, A., Andrade, A., Lamounier, E., Carrijo, R., 2003. The development of a virtual myoelectric prosthesis controlled by an EMG pattern recognition system based on neural networks. J. Int. Inf. Syst. 21 (2), 127–141.

Stegeman, D., Hermens, H. Standards for surface electromyography: The European project Surface EMG for non-invasive assessment of muscles (SENIAM). Enschede: Roessingh Research and Development 2007. pp. 108–112.

Topalović, I., Janković, M., Popović, D.B. Validation of the acquisition system Smarting for EMG recordings with electrode array. in: Proceedings of 2nd IcETRAN, Silver Lake, Serbia, June 8-11, 2015. MEI1.5.

Topalović, I., Popović, D.B. EMG maps for estimation of muscle activities during grasping. In: Proceedings of 3rd IcETRAN, Zlatibor, Serbia, June 12-15, 2016. MEI1.2.

Zwarts, M.J., Stegeman, D.F., 2003. Multichannel surface EMG: basic aspects and clinical utility. Muscle Nerve: Off. J. Am. Assoc. Electrodiag. Med. 28 (1), 1–17.

Ivan Topalović is a Ph.D. student at the School of Electrical Engineering, University of Belgrade, Belgrade, Serbia. He received his bachelor and master's degrees at the School of Electrical Engineering, the University of Belgrade with the specialization in biomedical engineering. He is currently a Research Assistant at the Institute of Technical Sciences of the Serbian Academy of Sciences and Arts. His Ph.D. project is in the domain of enhanced understanding and using of electrophysiological signals for the feedback, assessment of function and rehabilitation of persons with motor disability. The research is based on advanced methods of signals and image processing.